

ISTITUTO NAZIONALE DI FISICA NUCLEARE
Laboratori Nazionali di Frascati

LNF-84/70

Z.E.Mezzani et al.: COULOMB SUM RULE FOR ^{40}Ca , ^{48}Ca
AND ^{56}Fe FOR $|\vec{q}| \leq 550 \text{ MeV}/c$

Estratto da:
Phys. Rev. Letters 52, 2130 (1984)

Coulomb Sum Rule for ^{40}Ca , ^{48}Ca , and ^{56}Fe for $|\vec{q}| \leq 550 \text{ MeV}/c$

Z. E. Meziani, P. Barreau, M. Bernheim, J. Morgenstern, and S. Turck-Chieze
Service de Physique Nucléaire-Haute Energie, Centre d'Etudes Nucléaires de Saclay, F-91191 Gif-sur-Yvette Cedex, France

and

R. Altemus, J. McCarthy, L. J. Orphanos, and R. R. Whitney
Department of Physics University of Virginia, Charlottesville, Virginia 22901

and

G. P. Capitani and E. De Sanctis
*Laboratori Nazionali di Frascati, Istituto Nazionale di Fisica Nucleare,
 I-00044 Frascati, Roma Italy*

and

S. Frullani and F. Garibaldi
*Laboratorio della Radiazioni Istituto Superiore di Sanità, and Istituto Nazionale di Fisica Nucleare,
 Sezione Sanità, Roma, Italy*

(Received 4 April 1984)

Deep-inelastic electron scattering from ^{40}Ca , ^{48}Ca , and ^{56}Fe has been measured at 60° , 90° , and 140° and at inelasticities up to and including the $\Delta(3,3)$ region. Longitudinal response functions in the momentum interval $300 \text{ MeV}/c < |\vec{q}| < 600 \text{ MeV}/c$ were extracted. The experimental Coulomb sum rule is observed between the two calcium isotopes.

PACS numbers: 25.30.Fj

In high-energy electron-nucleus scattering at large momentum transfer, the quasidelectric peak dominates the spectrum. This peak exhibits broadening, reflecting the internal motion of the nucleons in the target, and its position corresponds approximately to elastic scattering from free nucleons. In previous experiments,¹ the position and the width of this peak have been used to extract the average nucleon binding energy and Fermi momentum of several nuclei. In order to isolate effects such as meson exchange currents, systematic studies have been performed recently on ^{56}Fe ,² ^{12}C ,³⁻⁵ and ^{40}Ca ,^{6,7} to separate the longitudinal response function from the transverse one in the quasifree region. Surprisingly, the longitudinal response, thought to be largely independent of mesonic degrees of freedom, is rather poorly reproduced, both in magnitude and shape, by a Fermi-gas calculation at momentum transfer as large as $410 \text{ MeV}/c$.⁸ This result suggests that a shell-model calculation including the distortion effects of the knock-out nucleon might improve the agreement with experiment. The interpretation of the experiment on ^{12}C (Ref. 5) shows the improvement quantitatively.

One of the tests of our understanding of the behavior of nucleons in the nuclear medium is expressed in terms of sum rules.⁹ It is believed that the Fourier transform of the two-body correlation vanishes at high momentum and, thus, that the Coulomb sum contains the total target charge

strength. This is true of the ^{12}C experiment of Ref. 5, whereas in the ^{56}Fe experiment of Ref. 2 the expected strength was not attained. This was one of our motivations to measure the cross sections and to extract the response functions of medium-weight nuclei up to a momentum transfer twice the Fermi momentum ($520 \text{ MeV}/c$), where no Pauli blocking occurs. Another aim was to examine the influence of neutron excess in the longitudinal response functions of the calcium isotopes.

In this Letter we present results from (e,e') measurements on ^{40}Ca , ^{48}Ca , and ^{56}Fe performed at the Saclay linear accelerator using the "600" spectrometer in the HE1 end station. In order to separate the longitudinal response function, data were collected at incident electron energies ranging from 120 to 695 MeV and at three scattering angles, 60° , 90° , and 140° .

The detector system, described in detail by Barreau *et al.*,⁵ and Leconte *et al.*,¹⁰ consisted of two multiwire proportional chambers, a plane of plastic scintillators, and a gas Čerenkov counter. The scintillation counters in coincidence with the Čerenkov counter provided the trigger for electrons. The electron detection efficiency was measured to be greater than 99% for electron final energy greater than 250 MeV.

Although most pion events were rejected, accidental coincidences between pions detected in the scintillators and background events in the Čerenkov

counter could still occur. In order to correct for such events, pion spectra were systematically measured. The correction was kept to less than 5% by adjusting the beam current when necessary. The contamination due to pair-produced electrons was negligible at high scattered electron energy but reached 10% at the lowest energy retained for the separations, 100 MeV. It was removed by reversing the magnetic field of the spectrometer and measuring the corresponding positrons.

The absolute efficiency of the detector was evaluated by measuring elastic cross sections from ^{12}C for incident energies ranging from 100 to 620 MeV and comparing the results with absolute measurements of Reuter *et al.*¹¹ When possible the momentum transfer was chosen to be near the second maximum of the form factor at $q \approx 2 \text{ fm}^{-1}$.

The data were corrected for radiative effects in two steps. The radiative tail of the elastic peak was first subtracted from measured spectra, and then an unfolding procedure was applied to the inelastic

(continuum) part of each spectrum in order to obtain the one-photon exchange cross sections. The radiative tail was computed following the "exact" formulation of Mo and Tsai.¹² At each angle the elastic form factors were calculated with a phase-shift code which made use of charge densities obtained in previous elastic-scattering experiments.¹³ The error made in using the first Born approximation to evaluate the radiative tail was estimated by Borie¹⁴ in the peaking approximation with the assumption of a point nucleus. This error amounts to about 15% of the calculated radiative tail, which led us to not use data if the magnitude of the tail was greater than 25% of the measured cross section. The continuum part of the spectra was corrected for radiative effects following the unfolding procedure developed by Miller.¹⁵ This is the standard analysis procedure followed in Ref. 1-7.

We present the separated response functions R_L as expressed in the plane-wave Born approximation by the following formula:

$$d\sigma/d\Omega d\omega = \sigma_M \{ (q_\mu/|\vec{q}|)^4 R_L(\vec{q}, \omega) + [\frac{1}{2}(q_\mu/|\vec{q}|)^2 + \tan^2 \frac{1}{2}\theta] R_T(\vec{q}, \omega) \},$$

$$\sigma_M = \left(\frac{\hbar c \alpha \cos \frac{1}{2}\theta}{2E_i \sin^2 \frac{1}{2}\theta} \right)^2, \quad q_\mu^2 = \omega^2 - \vec{q}^2,$$

where q_μ is the four-momentum, ω the energy transfer, E_i the incident energy, θ the laboratory scattering angle, and α the fine-structure constant. With measurements at three angles, the negligible effect of distortion was confirmed.

We show in Figs. 1(a) and 1(b) the longitudinal response functions of ^{40}Ca , ^{48}Ca , and ^{56}Fe at $|\vec{q}| = 410$ and $550 \text{ MeV}/c$. The experimental results are compared with three theoretical calculations. The one due to Van Orden¹⁶ (dashed line) uses a relativistic zero-temperature Fermi-gas model to describe the target ground state. The two parameters of this model, average separation energy ($\bar{\epsilon} = 36 \text{ MeV}$) and Fermi momentum ($k_F = 260 \text{ MeV}/c$ for ^{56}Fe and $k_F = 250 \text{ MeV}/c$ for $^{40,48}\text{Ca}$), have been taken from Ref. 1. One can clearly see that this model overestimates R_L whereas, as it is known, it predicts the total measured response function fairly well. The other calculation by Laget¹⁷ (solid line) uses the shell model with nucleon momentum distributions and separation energies derived from $(e, e'p)$ experiments.¹⁹ The final-state interaction of the knock-out nucleon is calculated with use of the real part of an optical potential. The agreement with the longitudinal response is clearly better. The third one by Do Dang¹⁸ at $410 \text{ MeV}/c$ (dot-dashed line) is a first at-

tempt to compute the electromagnetic interaction with a nucleon bound in infinite nuclear matter through scalar and vector Lorentz potentials which are generally used in Dirac phenomenology.²⁰ The ground state is described with a shell model. The only parameter in this model that is free, but that can be deduced from other studies,²⁰ is the link between the scalar potential and the nuclear density. This treatment agrees with the data at $|\vec{q}| = 410 \text{ MeV}/c$ and seems to be a promising way to simultaneously reproduce the longitudinal and the transverse response functions in the quasielastic region. Calculations at other momentum transfers are under way.

In order to compare the charge-scattering strength with the Coulomb sum rule based on a closure relation we have performed the integration of the longitudinal response function along paths of constant three-momentum transfer to obtain the Coulomb sum $C(q)$:

$$C(q) = \int_{0^+}^{\omega_{\max}} R_L(\vec{q}, \omega) d\omega,$$

where the 0^+ limit excludes elastic scattering and ω_{\max} is the experimental limit beyond which data are unreliable because of electron-pair contamination and detector inefficiency. We present in Fig. 2

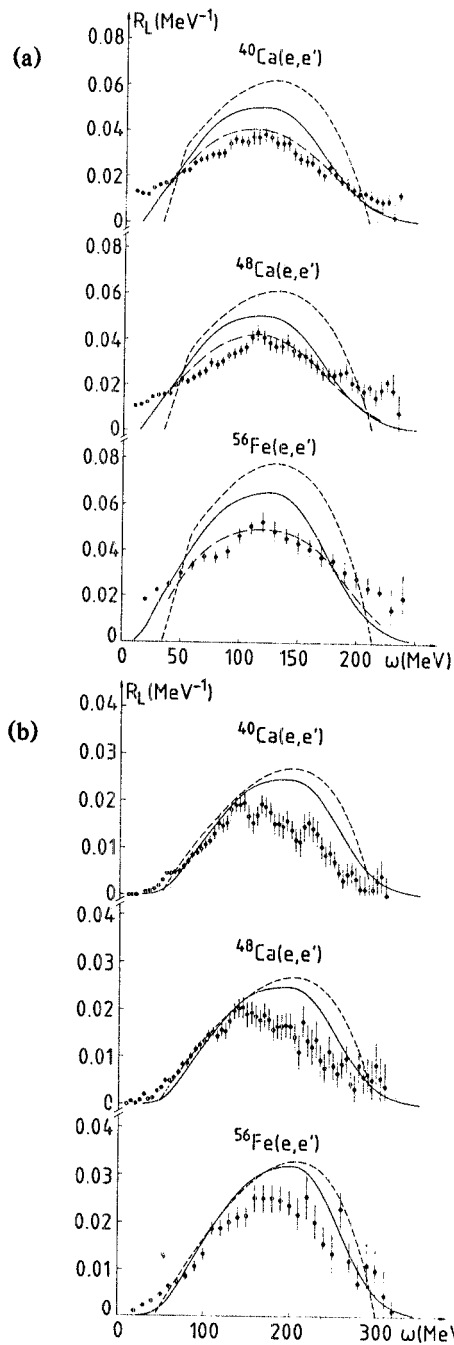


FIG. 1. The longitudinal response for ^{40}Ca , ^{48}Ca , and ^{56}Fe at (a) $|\vec{q}| = 410 \text{ MeV}/c$ and (b) $|\vec{q}| = 550 \text{ MeV}/c$. The dashed line is a Fermi-gas calculation by Van Orden (Ref. 16); the solid line, a shell model calculation by Laget (Ref. 17); and the dot-dashed line a calculation by Do Dang (Ref. 18).

experimental results for the Coulomb sum rule at momentum transfers between 330 and 550 MeV/c . These are compared to the calculations by Van Orden and Laget, in which the energy-loss cutoff in the integration is close to the experimental one (see Table I). As pointed out by Noble,²¹ most of the

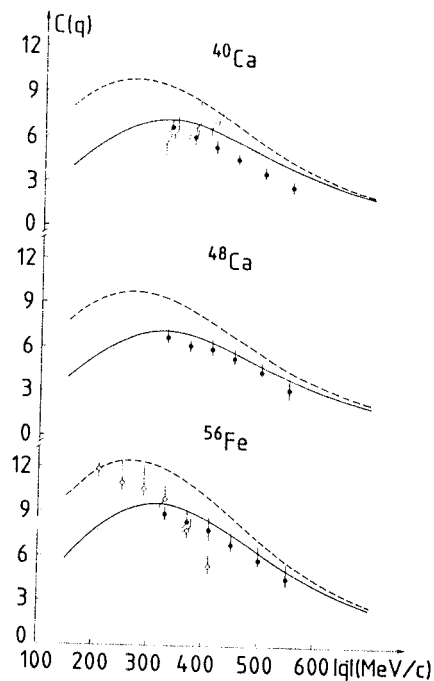


FIG. 2. Coulomb sum rule for ^{40}Ca , ^{48}Ca , and ^{56}Fe (full circles); calculations are the same as in Fig. 1. The errors shown include both statistical and systematic contributions. The open squares are data from Ref. 7; the open lozenges are data from Ref. 2.

single-particle strength is concentrated in the quasielastic region. However, within the limit of our integration in ω , the lack of strength is observed to be 30% in ^{40}Ca and 20% in both ^{48}Ca and ^{56}Fe . This situation is different from the ^{12}C case where the Coulomb sum is well saturated. Viollier and Walecka²² estimate the effect of two-body correlations to be at most 10% suppression in the region $|\vec{q}| = 2k_F$ corresponding to infinite nuclear matter ($k_F = 1.42 \text{ fm}^{-1}$). This effect is difficult to disentangle from the experimental point of view, because the sum rule needs an integration over an infinite range of excitation energy, while the experiment is limited by the physical region $\omega < |\vec{q}|$. On the other hand relativistic effects in the $e-N$ interaction can modify the sum rule substantially.²³

An interesting effect is observed when we compare the Coulomb sum of the two calcium isotopes. The ratio of the Coulomb sums evaluated over the same region of excitation energy (Table I) exhibits a slow increase in favor of ^{48}Ca with increasing momentum transfer. The order of this effect is 20% at $|\vec{q}| = 550 \text{ MeV}/c$, and neither Van Orden nor Laget predict an effect of this magnitude in the longitudinal response function due to the eight extra neutrons in ^{48}Ca . The recent relativistic calculation by Walecka, however, suggests this kind of ef-

TABLE I. Coulomb sum rule $C(|\vec{q}|)$ for ^{40}Ca , ^{48}Ca , and ^{56}Fe nuclei at the given momentum transfers $|\vec{q}|$ and energy losses ω_{max} . The ratio between the $C(|\vec{q}|)$ for the two calcium isotopes is also given.

$ \vec{q} $ (MeV/c)	ω_{max} (MeV)	$C(\vec{q})$ ^{40}Ca	$C(\vec{q})$ ^{48}Ca	Ratio 48/40	ω_{max} (MeV)	$C(\vec{q})$ ^{56}Fe
330	175	6.58 ± 0.56	6.66 ± 0.60	1.012 ± 0.038	160	8.85 ± 0.57
370	195	5.98 ± 0.55	6.14 ± 0.60	1.027 ± 0.039	180	8.36 ± 0.81
410	235	5.31 ± 0.62	5.92 ± 0.70	1.115 ± 0.042	240	7.83 ± 0.98
450	265	4.52 ± 0.64	5.29 ± 0.70	1.170 ± 0.044	260	6.85 ± 0.83
500	290	3.58 ± 0.68	4.43 ± 0.72	1.237 ± 0.047	310	5.86 ± 1.03
550	310	2.73 ± 0.56	3.19 ± 0.67	1.168 ± 0.049	350	4.6 ± 1.07

fect.²⁴ Great care was taken in testing the homogeneity of each isotope target (by absorption of 60-keV photons from a ^{241}Am source), because it is the main source of error in this kind of comparison.

In summary, we have measured deep-inelastic electron-scattering cross sections from ^{40}Ca , ^{48}Ca , and ^{56}Fe and separated the longitudinal part, R_L , of the total response function up to a momentum transfer $|\vec{q}| = 550 \text{ MeV}/c$. R_L exhibits features that the Fermi-gas model cannot explain at 410 MeV/c and higher momentum. This result is within quoted uncertainties but slightly different from the recently published result on ^{40}Ca (Ref. 7) where the Coulomb sum rule gives $(90 \pm 30)\%$ of the Fermi-gas prediction at this momentum transfer. The Coulomb sum rule was computed and shows a suppression of 30% for ^{40}Ca and of 20% for both ^{48}Ca and ^{56}Fe at a momentum transfer greater than twice the Fermi momentum. We have observed a difference in Coulomb sum rule between the two calcium isotopes.

We thank the technical staff of the Saclay linear accelerator for their support during this experiment. We thank the Ministry of Education and Scientific Research of Algeria for partial financial support. This work was also supported in part by the U.S. Department of Energy and the National Science Foundation.

with the results reported here.

³J. Mougey *et al.*, Phys. Rev. Lett. **41**, 1645 (1978).

⁴P. Barreau *et al.*, Nucl. Phys. **A358**, 287c (1981).

⁵P. Barreau *et al.*, Nucl. Phys. **A402**, 515 (1983).

⁶P. D. Zimmerman *et al.*, Phys. Lett. **80B**, 45 (1978).

⁷M. Deady *et al.*, Phys. Rev. C **28**, 631 (1983).

⁸J. W. Van Orden and T. W. Donnelly, Ann. Phys. (N.Y.) **131**, 451 (1981).

⁹S. D. Drell and C. L. Schwartz, Phys. Rev. **112**, 568 (1958).

¹⁰P. Leconte *et al.*, Nucl. Instrum. Methods **169**, 401 (1980).

¹¹W. Reuter *et al.*, Phys. Rev. C **26**, 806 (1982).

¹²L. W. Mo and Y. S. Tsai, Rev. Mod. Phys. **41**, 205 (1969); Y. S. Tsai, SLAC Report No. SLAC-PUB-848, 1971 (unpublished).

¹³I. Sick *et al.*, Phys. Lett. **88B**, 245 (1979), and references therein; J. Emrich *et al.*, Nucl. Phys. **A396**, 401c (1983); H. Thiessen *et al.*, Z. Phys. **231**, 475 (1970); C. W. de Karger *et al.*, At. Data Nucl. Data Tables **14**, 479 (1974).

¹⁴E. Borie, Lett. Nuovo Cimento **1**, 106 (1971).

¹⁵G. Miller, SLAC Report No. 129, 1971 (unpublished).

¹⁶J. W. Van Orden, Ph.D. thesis, Stanford University, 1978 (unpublished).

¹⁷J. M. Laget, *From Collective States to Quarks in Nuclei*, Lecture Notes in Physics Vol. 137, edited by H. Ahrénhovel and A. M. Saruis (Springer, Berlin, 1981), and private communication.

¹⁸G. Do Dang and Pham Vam Thiew, Phys. Rev. C **28**, 1845 (1983); G. Do Dang and Nguyen Van Giai, to be published.

¹⁹J. Mougey *et al.*, Nucl. Phys. **A262**, 461 (1976).

²⁰L. S. Celenza *et al.*, Phys. Rev. C **26**, 320 (1982); M. Jaminon and C. Mahaux, Phys. Rev. C **24**, 1353 (1981).

²¹J. V. Noble, Phys. Rev. C **27**, 423 (1983).

²²R. D. Viollier and J. D. Walecka, Acta Phys. Polon. B **8**, 1680 (1977).

²³T. de Forest, Jr., Nucl. Phys. **A392**, 232 (1983), and to be published.

²⁴J. D. Walecka, Nucl. Phys. **A399**, 387 (1983).

¹R. R. Whitney *et al.*, Phys. Rev. C **9**, 2330 (1974).

²R. Altemus *et al.*, Phys. Rev. Lett. **44**, 965 (1980). Not included in these data, taken at the Massachusetts Institute of Technology-Bates linac, was a then unknown contribution due to secondary scattering from the target chamber aperture. When this large W component of the cross section is accounted for, these data are consistent